Check for updates

View Article Online
View Journal

PCCP
Physical Chemistry Chemical Physics

Accepted Manuscript

This article can be cited before page numbers have been issued, to do this please use: Y. Liu, A. Li, Z. Ma, W. Xu, Z. Ma and X. Jia, *Phys. Chem. Chem. Phys.*, 2020, DOI: 10.1039/D0CP02783A.

Volume 19
Number 1
7 January 2017
Pages 1-896

PCCP
Physical Chemistry Chemical Physics
rsc.li/pccp

ISSN 1463-9076

ROYAL SOCIETY OF CHEMISTRY

PAPER
H.-P. Loock *et al.*
Determination of the thermal, oxidative and photochemical degradation rates of scintillator liquid by fluorescence EEM spectroscopy

This is an Accepted Manuscript, which has been through the Royal Society of Chemistry peer review process and has been accepted for publication.

Accepted Manuscripts are published online shortly after acceptance, before technical editing, formatting and proof reading. Using this free service, authors can make their results available to the community, in citable form, before we publish the edited article. We will replace this Accepted Manuscript with the edited and formatted Advance Article as soon as it is available.

You can find more information about Accepted Manuscripts in the Information for Authors.

Please note that technical editing may introduce minor changes to the text and/or graphics, which may alter content. The journal's standard Terms & Conditions and the Ethical guidelines still apply. In no event shall the Royal Society of Chemistry be held responsible for any errors or omissions in this Accepted Manuscript or any consequences arising from the use of any information it contains.

ROYAL SOCIETY OF CHEMISTRY

rsc.li/pccp

Journal Name

Physical Chemistry Chemical Physics

Dynamic Article Links ►

View Article Online
DOI: 10.1039/D0CP02763A

Cite this: DOI: 10.1039/c0xx00000x

www.rsc.org/xxxxxx

ARTICLE TYPE

Multicolored Fluorescence Variation of a New Carbazole-Based AIEE Molecule by External Stimuli

Yan Liu,[ae] Aisen Li,[be] Zhimin Ma,[c] Weiqing Xu,[b] Zhiyong Ma,*[a] and Xinru Jia[d]

Received (in XXX, XXX) Xth XXXXXXXXX 20XX, Accepted Xth XXXXXXXXX 20XX
DOI: 10.1039/b000000x

In this article, we design and synthesize a new carbazle-based molecule Cz2CN with twisted D-A structure, using carbazole group as the donor and dicyanoethylene fragment as the acceptor. Such twisted D-A structure endows Cz2CN with two characteristic emission bands, LE emission and ICT emission. Cz2CN is enabled with AIEE, solvatochromism, different response to anisotropic shearing force and isotropic hydrostatic pressure, due to the sensitivity of ICT emission to aggregation, solvent polarity and mechanical force. Aggregation benefits the ICT emission, leading to the AIEE of Cz2CN in THF/water system. Polar solvent can help stabilize the ICT excited states and make the ICT emission red shift. The original crystalline powder is strongly fluorescent with high quantum yield of 40.4%. The single crystal of Cz2CN is obtained and dimers without π-π interactions among carbazole groups contribute to the strong emission. Anisotropic shearing alters the emission of Cz2CN powder from sky blue (474 nm) to green (520 nm). The single crystal of Cz2CN undergoes a distinct multicolored variation from sky-blue (476 nm) to green (510 nm) and further to orange (590 nm) by isotropic hydrostatic pressure. The emission of the original powder/crystal is dominant by LE emission in HLCT. Upon force/pressure, the ICT emission becomes dominated and red shifts progressively. To the best of our knowledge, Cz2CN is an interesting carbazole-based molecule that shows simultaneous AIEE, solvatochromism and force-induced multicolored variation.

Introduction

Smart organic luminescence materials mean that such materials can respond to external stimuli and give out some signal.[1-3] Solid-state smart organic materials with adjustable and stimuli-responsive luminescence have been drawing considerable attention due to their broad applications in organic light-emitting diodes, sensors, display systems, anti-counterfeiting and data storage.[4-8] However, many organic π-conjugated molecules with strong fluorescence in solution become non-fluorescent in the solid state because of the notorious aggregation caused quenching (ACQ).[9, 10] In 2001, Prof. Tang discovered the aggregation-induced emission enhancement (AIEE) and provided a new strategy to develop strongly emissive solids by tuning nonplanar molecular structure and regulating supramolecular interactions.[11-16] Carbazole, as an important luminescence group, has to be faced with ACQ owing to its coplanar structure, which hampers its wide application. How to acquire carbazole-based luminescent molecules with AIEE is challenging and needs to be solved.

Mechanical force, as an easily obtainable and eco-friendly stimulus, can perturb the molecular orientation, molecular conformation and intermolecular interactions and finally lead to an emission color change.[17-19] Mechanical force includes different forms, for example, grinding, shearing, stretching, tension and hydrostatic pressure.[20-30] Some force-responsive carbazole derivatives have been reported.[31-39] However, there is nearly no literature that has reported that carbazole derivatives show responsiveness to both anisotropic shearing force and isotropic hydrostatic pressure, although these factors are of great significance in the applications of these materials.

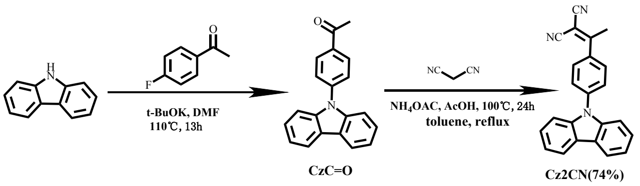

Scheme 1. The synthetic route of **Cz2CN**.

Carbazole group is widely utilized as an electron donor to fabricate luminogens.[40-43] As reported, luminogens with twisted donor-acceptor (D-A) structure often show unique energy band owing to the existence of intercrossed hybridized local and charge transfer (HLCT) excited state.[44-51] Modifying the electron acceptor and the conjugated spacer between donor and acceptor can easily change the luminescent features of D-A molecules.[46, 52]It is well known that restriction of intramolecular motions (RIM) is proposed as the mechanism for the AIE/AIEE effect, so AIEE luminogens glow weakly in dilute solution due to intramolecular motion but become highly emissive in solid state because the intermolecular π-π stacking is avoided, and the twisted geometry help in reducing the π-π staking interaction. Hence, our design concept is to introduce highly twisted acceptor to prevent the whole molecules from being too close and finally to achieve

AIEE. Meanwhile, the molecular conformation and the intermolecular interaction can be disturbed by mechanical force, leading to the ICT emission shift and finally achieving multicolored switch. [45, 53-56]

In this article, we design and synthesize a new carbazle-based molecule Cz2CN with twisted D-A structure, using carbazole group as the donor and dicyanoethylene fragment as the acceptor. Such twisted D-A structure endows Cz2CN with two characteristic emission bands, LE emission and ICT emission. Cz2CN is enabled with AIEE, solvatochromism, different response to anisotropic shearing force and isotropic hydrostatic pressure, due to the sensitivity of ICT emission to aggregation, solvent polarity and mechanical force. Aggregation benefits the ICT emission, leading to the AIEE of Cz2CN in THF/water system. Polar solvent can help stabilize the ICT excited states and make the ICT emission red shift. The original crystalline powder is strongly fluorescent with high quantum yield of 40.4%. The single crystal of Cz2CN is obtained and unique dimers without π-π interactions among carbazole groups contribute to the strong emission. Anisotropic shearing alters the emission of Cz2CN powder from sky blue (474 nm) to green (520 nm). The single crystal of Cz2CN undergoes a distinct multicolored variation from sky-blue (476 nm) to green (510 nm) and further to orange (590 nm) by isotropic hydrostatic pressure. The emission of the original powder/crystal is dominant by LE emission in HLCT. Upon force/pressure, the ICT emission becomes dominated and red-shifts progressively. To the best of our knowledge, Cz2CN is an interesting carbazole-based molecule that shows simultaneous AIEE, solvatochromism and force-induced multicolored variation. This study is expected to pave a new way for further understanding the relationship between the D-A molecular structure and stimuli-responsive properties and lay the foundation for their application.

Results and discussion

The target molecule Cz2CN is composed of a carbazole group and a dicyanoethylene fragment bridged by a benzene ring. CzC=O was gained *via* the typical aromatic nucleophilic substitution reaction between carbazole and 1-(4-fluorophenyl)ethan-1-one. Cz2CN was acquired as a light yellow powder with a yield of 74% by a typical condensation reaction, keeping CzC=O and malononitrile in the solvent of acetic acid at 100 °C for 24 h. The molecular structure and geometry of Cz2CN is confirmed by ^{1}H NMR, ^{13}C NMR, HR-MS and single crystal data. The synthetic procedures and the molecular characterization are available in the Supporting Information (Scheme 1, Figure S1-S3, Table S1).

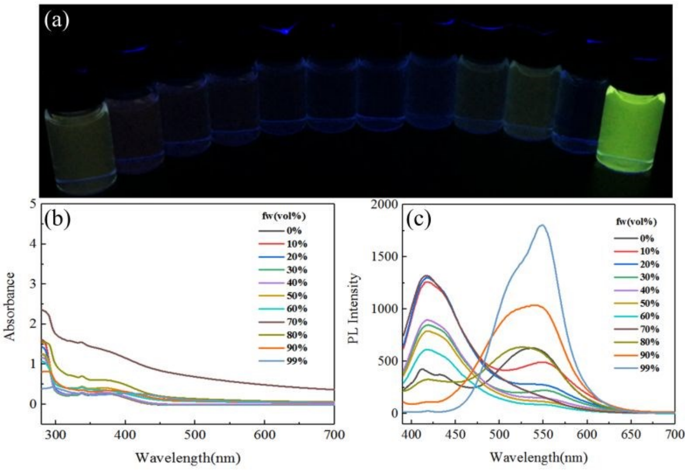

Figure 1. (a) Fluorescent images of **Cz2CN** in mixed solvents of THF/water with different water fraction (fw) under 365 nm UV light; (b) UV-Vis absorption and (c) fluorescence (λ_{ex}=365 nm) spectra of **Cz2CN** (20 μM) in THF/water mixtures with different fw.

As well-known, carbazole tends to form π-π interaction due to its coplanar structure, which is detrimental to strong fluorescence in the solid state. Unexpectedly, Cz2CN displays remarkable aggregation-induced emission enhancement (AIEE) property (Figure 1a&Figure S4). We carried out fluorescence and absorption spectra to verify the AIEE activity. In the diluted THF solution, the maximum absorption band and the emission peak of Cz2CN were located at 275 nm and ~415 nm (average lifetime, τ_a= 1.40 ns), respectively. When lifting the water fraction (f_w), the Mie scattering effect was observed in the absorption spectra, revealing that aggregated particles took shape (Figure 1b). As f_w increased, the emission at 415 nm weakened while a new emission band at 550 nm (τ_a=4.71 ns, Figure S5) appeared and enhanced gradually (Figure 1c). The dynamic light scattering (DLS) study was performed on the solution of Cz2CN in 99% water/THF(v/v) to investigate the particle size distribution. As shown in Figure S6, and one can note that their sizes are concentrated at 312.3 nm in average, indicating that the emission enhancement of Cz2CN originates from the formation of nanoaggregates. According to our previous work,[55-57] the 415 nm emission and the 550 nm emission are attributed to the LE emission of carbazole and ICT emission, respectively. Obviously, the D-A system of Cz2CN are both ICT-active and AIEE-active. Upon gradual addition of water (as a poor solvent), significant aggregation occurs and the AIEE effect dominates the ICT effect with the consequence that the ICT emission at 550 nm rises (Figure 1c). Therefore, aggregation prohibited the non-radiation channels and benefited the ICT emission, finally resulting in the strong fluorescence with high quantum yield (Table S2).

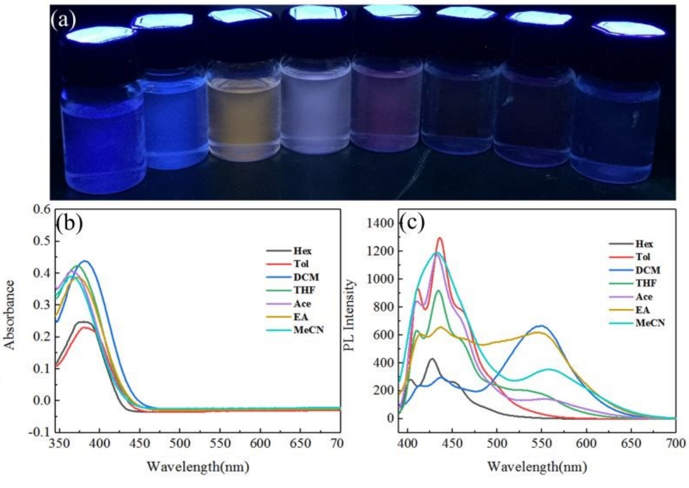

Figure 2. (a) Fluorescent images of **Cz2CN** in different organic solvent under 365 nm UV light; (b) UV-Vis absorption and (c) fluorescence (λ_{ex}=365 nm) spectra of **Cz2CN** (20 μM) in different organic solvent.

Cz2CN is featured with a Donor-Acceptor structure. Firstly, quantum mechanical computations *via* DFT method were performed to gain the highest occupied molecular orbital (HOMO) and the lowest unoccupied molecular orbital (LUMO) of Cz2CN (Figure S7). The electron cloud of the HOMO is distributed at the carbazole group while that of the LUMO is mainly confined over the dicyanoethylene fragment, indicating that Cz2CN has a separated D-A structure, which enables the molecule to undergo a

View Article Online
DOI: 10.1039/D0CP02783A

typical ICT process. Secondly, we tested the photophysical property in different organic solvent (Figure 2a), and the corresponding data were illustrated in Table S3. In dichloromethane, THF, acetone, ethanol and acetonitrile, the ICT emission of Cz2CN was detected at ~550 nm (Figure S8) and the intensities differed widely (Figure 2c). As documented,[45] ICT emission is highly sensitive to external environment, which is in consistence with our data. In this case, the ICT process is also allergic to solvent polarity but shows something different. To better evaluate the effects of solvents on the emission features, the relationship between the solvent polarity parameter and the Stokes shift according to the Lippert-Mataga plot was investigated (Figure S9), which displays an almost linear correlation of the Stokes shift with solvent polarity, reflecting the larger charge separation and higher dipole moment in the excited state than in the ground state. Even though Cz2CN showed solvatochromism, the ICT emission was quite weak in polar solvents due to free intramolecular motion. Given the AIEE property of Cz2CN, intensity of ICT emission much more depends on the aggregation state than the solvent polarity. It is worth noting that Cz2CN is an interesting D-A molecule that possesses both AIEE property and solvatochromism.

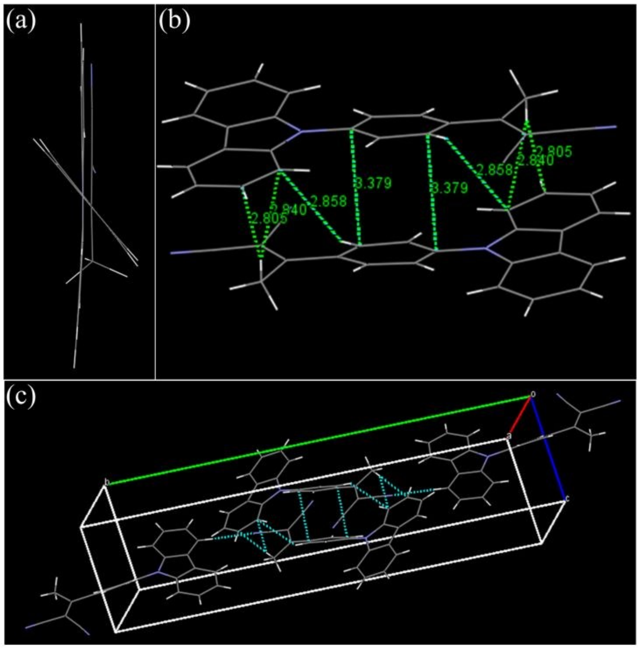

Figure 3. (a) The molecular geometry of **Cz2CN**; (b) the unique dimer with strong interactions and (c) the unit cell in the single crystal. White：Hydrogen, Grey：Carbon, Blue: Nitrogen.

Interestingly, Cz2CN demonstrated strong solid-state luminescence. The original crystalline powder was obtained from vacuum evaporation and gave out shiny sky-blue fluorescence. The emission band was centred at 474 nm; the quantum yield was quite high and calculated to be 40.4%. Generally, the solid-stated luminescent property is closely relevant to the stacking mode. Luckily, the single crystal of Cz2CN was successfully cultivated by slow evaporation of petroleum ether into the dichloromethane solution. Cz2CN crystallizes according to the space group of *P 1 21/c 1* (No. 14) and the single crystal is in the monoclinic crystal system with four molecules in each unit cell (Figure 3c, Figure S10, S11&S12). The dihedral angle between carbazole group and benzene ring is 40.0° and Cz2CN adopts a twisted geometry (Figure 3a). Obviously, a kind of dimer in a head-tail packing style forms in the single crystal. Viewing along a axis and c axis, the dimers can be observed clearly (Figure S10&S12). There are strong interactions between the carbazole group (head) and the dicyanoethylene fragment (tail) (Figure 3b), such as C-H…π (2.805 Å and 2.840 Å). The spacer benzene ring interacts with each other *via* enhanced π-π interactions (3.379 Å, 3.379 Å) and also displays interaction with carbazole through C-H…π (2.858 Å). However, no interaction among carbazole groups is observed. The unique dimer structure can confine the molecular motion due to the strong intermolecular interations and also prevent excitons from quenching by keeping the whole molecules from being too close, leading to strong light emission. In addition, the methyl groups effectively decrease the fractional of free volumes within the crystal lattice and subsequently suppress the non-radiative decay pathways of the excited structural relaxation.

Cz2CN shows solid-state stimuli-responsive property. The mechanofluochromic data are summarized in Table S4.As depicted above, emission of the original powder was located at 474 nm with a sky-blue color (quantum yield: Φ=0.404). The emission band had a short lifetime of 7.01 ns (Figure S14a), assigned to prompt fluorescence. The powder of Cz2CN was sensitive to external force. When shearing by a blunt pestle, the emission red-shifted to 520 nm (Φ=0.214) with a brilliant green and became broad. The new emission band was also ascribable to prompt fluorescence due to its short lifetime of 3.53 ns (Figure S14b). Why the quantum yield decreased after shearing was probably due to that π-π interactions formed among carbazole groups. Moreover, there are many intermolecular interactions among crystalline powder so that the nonradiative relaxation channel is prohibited, finally resulting in a high quantum yield. Meanwhile, the nonradiative decay rate (k_{nr}) of Cz2CN powder increased a lot (from $82.37\times10^{6}\ S^{-1}$ to $219.38\times10^{6}\ S^{-1}$) by simply grinding, so the QY of the ground powder decreased.The green color would be totally restored to the original sky-blue and the 474 nm emission band appeared again after being treated by dichloromethane vapor (Figure 4a-d). Thus, the abovementioned data unearth that Cz2CN displays reversible mechanofluochromic behavior. We deduced that the fluorescence at 474 nm and the fluorescence at 520 nm were both attributed to the hybridized local and charge transfer excited emission band (HLCT). This assumption would be discussed in detail hereinafter.

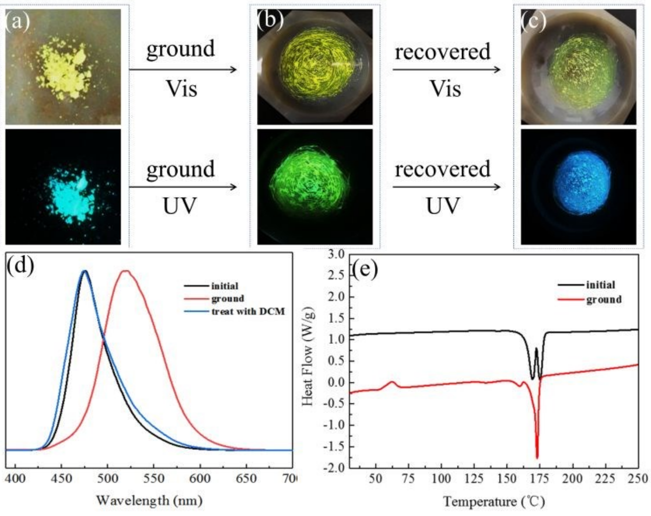

Figure 4. Optical images of (a) original sky-blue powder, (b) green powder after shearing, (c) restored powder by DCM vapor; the upper is under room light; the bottom is under UV light. (d) Fluorescent spectra of original powder (black line), powder after grinding (red line) and restored sample (blue line); (e) DSC

View Article Online
DOI: 10.1039/D0CP02783A

curves of the original powder, the ground powder.

To gain sight into the mechanochromic mechanism, X-ray diffraction (XRD) and differential scanning calorimetry (DSC) were carried out to explore the microstructure variation. For the original powder, a number of sharp scattering peaks were detected and these peaks were consistent with the simulated pattern based on the single crystal data, suggesting that the original powder has identical packing mode with the single crystal. The molecular structure of Cz2CN was stuck in the twisted geometry. In this regard, the LE emission was dominated in the HLCT emission. After shearing, these sharp peaks disappeared and phase transition occurred from crystalline form to amorphous state, resulting in the planarization of Cz2CN. Planarization is conducive to the ICT emission, leading to the red shift. Upon treatment of DCM vapor, the XRD pattern would return to the original state (Figure S15). DSC thermograms further evidenced the phase transition. The original powder exhibited two endothermic peaks at 168 ^{o}C and 175 ^{o}C, implying an unexpected crystal-crystal transition. After grinding, a new cold-recrystallization peak appeared at 63 ^{o}C and two endothermic peaks at 160 ^{o}C and 171 ^{o}C (Figure 4e, Figure S16&S17).

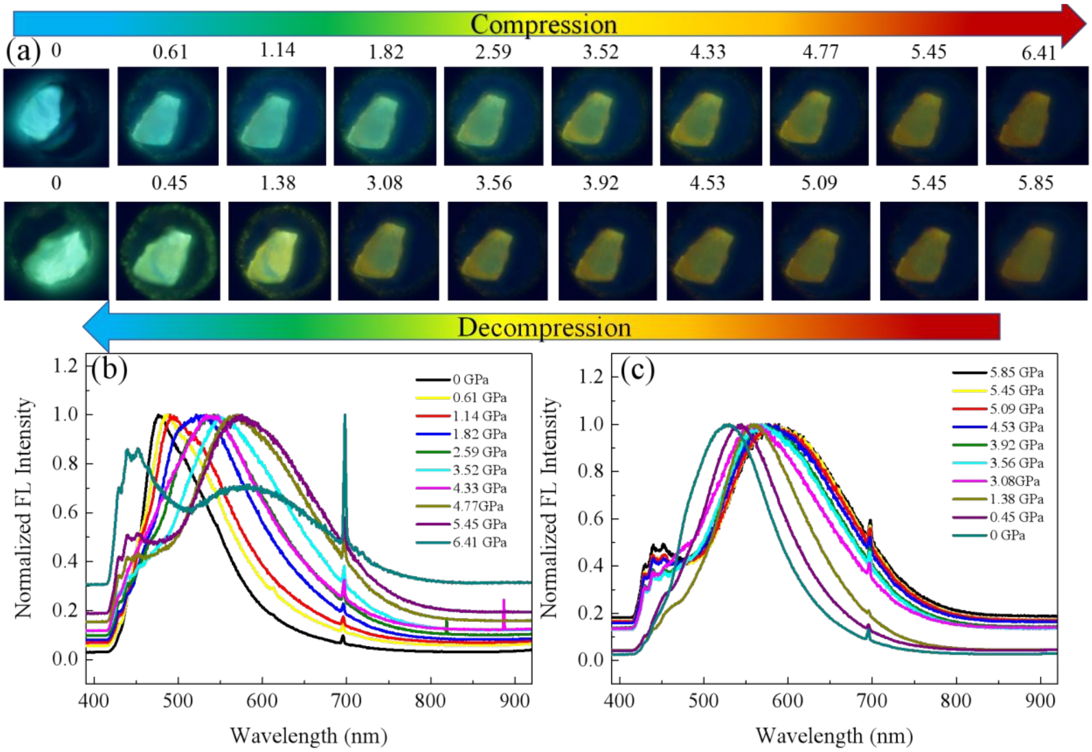

Figure 5. (a) Fluorescent images of the Cz2CN single crystal at different pressure. The corresponding normalized fluorescent spectra of the Cz2CN single crystal during (b) compression, (c) decompression.

To clearly see the mechanofluochromism of **Cz2CN** and quantify the relationship between the emission shift and the external force, the single crystal sample was subjected to high pressure by using the diamond anvil cell (DAC) device with silicone oil as the pressure-transmitting medium (PTM). *In-situ* fluorescence spectra and *in-situ* micrographs under different pressures were recorded to dynamically observe the color alteration. Remarkably, Cz2CN demonstrated fascinating pressure responsiveness. The single crystal underwent a distinct multicolored variation from sky-blue to green and further to orange when the hydrostatic pressure increased (Figure 5a). Initially, the sample afforded a dominant sky-blue fluorescence at 476 nm, in accordance with the original powder sample. The emission wavelength change could be divided into two stages. At the first stage, when the pressure was below 2.59 GPa, the emission wavelength gradually shifted from 476 nm to 510 nm. At the second stage, when further lifting the pressure, the emission band could split into two parts. A new group of emission peaks at ~450 nm developed and the position kept unchanged while the long-wavelength emission still red-shifted. The new short-wavelength emission should be the LE emission of carbazole groups because of its dull responsive to pressure. The long-wavelength emission could be ascribed to the ICT emission due to the D-A structure of Cz2CN and eventually reached 590 nm. It is rational that the increasing pressure compels the adjacent molecules to approach much closer and makes the molecular geometry of Cz2CN more planarized, leading to the red shift of ICT emission. The emission split originates from the separation of hybridized local and charge transfer excited states. When the high pressure was released, the emission split disappeared and the overall fluorescence could not return to 476 nm (Figure 5b&5c and Figure S18), indicating that the high pressure would damage

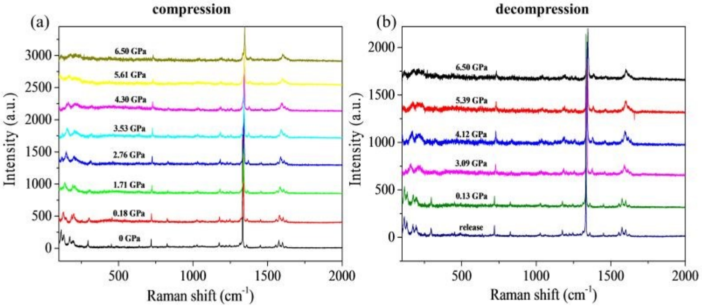

Figure 6. Raman spectra of **the Cz2CN** single crystal during (a) the compression process and (b) the decompression process.

View Article Online
DOI: 10.1039/D0CP02783A

To monitor the molecular-level change, we conducted high-pressure Raman spectra to monitor the Cz2CN single crystal. The Raman spectra could track the molecular structure changes during compression within the wavenumber range from 200 cm^{-1} to 2000 cm^{-1}. As shown in Figure 6, most Raman vibration modes exhibited blue-shifts as expected because of the decreased interatomic distances and the increased effective force constants upon compression.[58, 59] When the pressure was increased to 6.50 GPa, no new Raman peaks appeared and all the Raman peaks were retained, implying that only conformation change not phase transition occur during the compression process. The increasing pressure is not able to change the molecular structure of Cz2CN. Once the pressure returned to atmosphere, the measured Raman spectrum was identical with the original one (Figure S19), suggesting the conformational change is reversible.

Based on the above results, several key points can be concluded. (1) Cz2CN possesses two characteristic emissions, the LE emission and the ICT emission, due to the twisted D-A structure. (2) The ICT emission is more sensitive to the external environment, such as solvent polarity, aggregation; particularly, aggregation can enhance the ICT emission of Cz2CN. (3) The solid-state emission color change upon force/pressure is dominated by ICT emission, because mechanical stimuli is more likely to disturb the intermolecular interactions and molecular conformation which are both closely related to the ICT emission.

Conclusions

In summary, we report a newly designed molecule Cz2CN with twisted D-A structure. Cz2CN shows fascinating AIEE, solvatochromism and force-induced multicolored variation. The unique stimuli-responsive properties stem from HLCT emission of Cz2CN composed of LE component and ICT component. In particular, ICT emission of Cz2CN is susceptive to external stimuli and is dominated in the emission enhancement and color change. This study may open a new strategy to provide a broad perspective for the development of stimuli-responsive AIEE materials.

Acknowledgments

This work is financially supported by the Beijing Natural Science Foundation (2182054), the National Natural Science Foundation of China (21704002), the Big Science Project from BUCT (XK180301), and the Fundamental Research Funds for the Central Universities to Z. Y. Ma.

Notes and references

[a] *Beijing State Key Laboratory of Organic-Inorganic Composites, College of Chemical Engineering, Beijing University of Chemical Technology, Beijing 100029, China. E-mail: mazhy@mail.buct.edu.cn*

[b] *State Key Laboratory for Supramolecular Structure and Materials, Institute of Theoretical Chemistry, College of Physics, Jilin University, Changchun 130012, China.*

[c] *National high-tech industrial development zone in Jingdezhen, Jingdezhen, 333000, China.*

[d] *Beijing National Laboratory for Molecular Sciences, Key Laboratory of Polymer Chemistry and Physics of the Ministry of Education, College of Chemistry and Molecular Engineering, Peking University, Beijing 100871, China.*

[e] *These authors contributed equally.*

† Electronic Supplementary Information (ESI) available: [details of experimental sections, including synthesis, characterization, spectra, SAXSS patterns and optical images]. See DOI: 10.1039/b000000x/

1. M. Martinez-Abadia, R. Gimenez and M. B. Ros, *Adv. Mater*, 2018, **30**, 1704161.
2. Y. Sagara, S. Yamane, M. Mitani, C. Weder and T. Kato, *Adv. Mater*, 2016, **28**, 1073-1095.
3. X. Liu, A. Li, W. Xu, Z. Ma and X. Jia, *Materials Chemistry Frontiers*, 2019, **3**, 620-625.
4. H. J. Kim, D. R. Whang, J. Gierschner, C. H. Lee and S. Y. Park, *Angew. Chem. Int. Ed*, 2015, **54**, 4330-4333.
5. S. Mukherjee and P. Thilagar, *Angew. Chem. Int. Ed*, 2019, **58**, 7922-7932.
6. Z. Ma, M. Teng, Z. Wang, S. Yang and X. Jia, *Angew. Chem. Int. Ed*, 2013, **52**, 12268-12272.
7. Z. Ma, Z. Wang, X. Meng, Z. Ma, Z. Xu, Y. Ma and X. Jia, *Angew. Chem. Int. Ed*, 2016, **55**, 519-522.
8. L. Huang, Y. Qiu, C. Wu, Z. Ma, Z. Shen and X. Jia, *J. Mater. Chem. C*, 2018, **6**, 10250-10255.
9. J. Mei, Y. Hong, J. W. Lam, A. Qin, Y. Tang and B. Z. Tang, *Adv. Mater*, 2014, **26**, 5429-5479.
10. J. Mei, N. L. C. Leung, R. T. K. Kwok, J. W. Y. Lam and B. Z. Tang, *Chem.Rev*, 2015, **115**, 11718–11940.
11. D. Dang, Z. Qiu, T. Han, Y. Liu, M. Chen, R. T. K. Kwok, J. W. Y. Lam and B. Z. Tang, *Adv. Funct. Mater*, 2018, **28**, 1707210.
12. G. Huang, Y. Jiang, S. Yang, B. S. Li and B. Z. Tang, *Adv. Funct. Mater*, 2019, **29**, 1900516.
13. B. Huang, W. C. Chen, Z. Li, J. Zhang, W. Zhao, Y. Feng, B. Z. Tang and C. S. Lee, *Angew. Chem. Int. Ed*, 2018, **57**, 12473-12477.
14. H. Q. Peng, X. Zheng, T. Han, R. T. K. Kwok, J. W. Y. Lam, X. Huang and B. Z. Tang, *J. Am. Chem. Soc*, 2017, **139**, 10150-10156.
15. J. Wang, J. Mei, R. Hu, J. Z. Sun, A. Qin and B. Z. Tang, *J. Am. Chem. Soc*, 2012, **134**, 9956-9966.
16. N. Jiang, T. Shen, J. Z. Sun and B. Z. Tang, *Science China Materials*, 2019, **62**, 1227-1235.
17. Z. Chi, X. Zhang, B. Xu, X. Zhou, C. Ma, Y. Zhang, S. Liu and J. Xu, *Chem. Soc. Rev*, 2012, **41**, 3878-3896.
18. Y. Li, Z. Ma, A. Li, W. Xu, Y. Wang, H. Jiang, K. Wang, Y. Zhao and X. Jia, *ACS Appl Mater Interfaces*, 2017, **9**, 8910-8918.
19. Z. Ma, Z. Wang, M. Teng, Z. Xu and X. Jia, *Chemphyschem*, 2015, **16**, 1811-1828.
20. L. Wang, K. Wang, B. Zou, K. Ye, H. Zhang and Y. Wang, *Adv. Mater*, 2015, **27**, 2918-2922.
21. X. Wang, H. Zhang, R. Yu, L. Dong, D. Peng, A. Zhang, Y. Zhang, H. Liu, C. Pan and Z. L. Wang, *Adv. Mater*, 2015, **27**, 2324-2331.
22. X. Wang, Q. Liu, H. Yan, Z. Liu, M. Yao, Q. Zhang, S. Gong and W. He, *Chem. Commun* 2015, **51**, 7497-7500.
23. Q. Sui, X. T. Ren, Y. X. Dai, K. Wang, W. T. Li, T. Gong, J. J. Fang, B. Zou, E. Q. Gao and L. Wang, *Chemical Science*, 2017, **8**, 2758-2768.
24. Z. Ma, X. Meng, Y. Ji, A. Li, G. Qi, W. Xu, B. Zou, Y. Ma, G. C. Kuang and X. Jia, *Dyes and Pigments*, 2019, **162**, 136-144.
25. J. Sun, J. Han, L. Yang, Y. Duan, T. Han and Y. Jing, *J. Mater. Chem. C*, 2016, **4**, 8276-8283
26. B. Shao, R. Jin, A. Li, Y. Liu and W. Tian, *J. Mater. Chem. C*, 2019, **7**, 3263-3268
27. Y. Liu, Q. Zeng, B. Zou, Y. Liu and W. Tian, *Angew. Chem. Int. Ed*, 2018, **57**, 15907-15907.
28. Y. Sagara, T. Mutai, I. Yoshikawa and K. Araki, *J. Am. Chem. Soc*, 2007, **129**, 1520-1521.
29. X. Liu, C. Ma, A. Li, W. Xu, Z. Ma and X. Jia, *J. Mater. Chem. C*, 2019, **7**, 8398-8403
30. Z. Wang, Z. Ma, Y. Wang, Z. Xu, Y. Luo, Y. Wei and X. Jia, *Adv. Mater*, 2015, **27**, 6469-6474.
31. P. Z. Chen, H. Zhang, L. Y. Niu, Y. Zhang, Y. Z. Chen, H. B. Fu and Q. Z. Yang, *Adv. Funct. Mater*, 2017, **27**, 1700332.

DOI: 10.1039/D0CP02783A

32. X. Zhao, Y. Wu, N. Shi, X. Li, Y. Zhao, M. Sun, D. Ding, H. Xu and L. Xie, *Chin. J. Chem*, 2015, **33**, 955-960.
33. L. Huang, J. Liu, L. Liu, Q. Yang, Z. Ma and X. Jia, *Dyes and Pigments*, 2020, **173**, 107963.
34. X. Mei, K. Wei, G. Wen, Z. Liu, Z. Lin, Z. Zhou, L. Huang, E. Yang and Q. Ling, *Dyes and Pigments*, 2016, **133**, 345-353.
35. Y. Zhang, Y. Ma, L. Kong, Y. Tian and J. Yang, *Dyes and Pigments*, 2018, **159**, 314-321.
36. P. Z. Chen, J. X. Wang, L. Y. Niu, Y. Z. Chen and Q. Z. Yang, *J. Mater. Chem. C*, 2017, **5**, 12538-12546.
37. P. Wen, Z. Gao, R. Zhang, A. Li, F. Zhang, J. Li, J. Xie, Y. Wu, M. Wu and K. Guo, *J. Mater. Chem. C*, 2017, **5**, 6136-6143.
38. Y. Wang, G. Zhang, W. Zhang, X. Wang, Y. Wu, T. Liang, X. Hao, H. Fu, Y. Zhao and D. Zhang, *Small*, 2016, **12**, 6554-6561.
39. L. Huang, L. Liu, X. Li, H. Hu, M. Chen, Q. Yang, Z. Ma and X. Jia, *Angew. Chem. Int. Ed*, 2019, **58**, 16445-16450.
40. N. Gan, X. Wang, H. Ma, A. Lv, H. Wang, Q. Wang, M. Gu, S. Cai, Y. Zhang, L. Fu, M. Zhang, C. Dong, W. Yao, H. Shi, Z. An and W. Huang, *Angew. Chem. Int. Ed*, 2019, **58**, 14140-14145.
41. Y. Xiong, Z. Zhao, W. Zhao, H. Ma, Q. Peng, Z. He, X. Zhang, Y. Chen, X. He, J. W. Y. Lam and B. Z. Tang, *Angew. Chem. Int. Ed*, 2018, **57**, 7997-8001.
42. B. Prusti and M. Chakravarty, *ACS Omega*, 2019, **4**, 16963-16971.
43. B. Wex and B. R. Kaafarani, *J. Mater. Chem. C*, 2017, **5**, 8622-8653.
44. S. Sasaki, G. P. C. Drummen and G.-i. Konishi, *J. Mater. Chem. C*, 2016, **4**, 2731-2743.
45. A. Li, Z. Ma, J. Wu, P. Li, H. Wang, Y. Geng, S. Xu, B. Yang, H. Zhang, H. Cui and W. Xu, *Advanced Optical Materials*, 2018, **6**, 1700647.
46. Y. Zhang, K. Wang, G. Zhuang, Z. Xie, C. Zhang, F. Cao, G. Pan, H. Chen, B. Zou and Y. Ma, *Chem.-Eur. J.*, 2015, **21**, 2474-2479.
47. X. Liu, A. Li, W. Xu, Z. Ma and X. Jia, *PCCP*, 2018, **20**, 13249-13254.
48. W. Li, Y. Pan, L. Yao, H. Liu, S. Zhang, C. Wang, F. Shen, P. Lu, B. Yang and Y. Ma, *Adv. Opt. Mater*, 2014, **2**, 892-901.
49. Z. Wang, Y. Feng, S. Zhang, Y. Gao, Z. Gao, Y. Chen, X. Zhang, P. Lu, B. Yang, P. Chen, Y. Ma and S. Liu, *PCCP*, 2014, **16**, 20772-20779.
50. L. Yao, S. Zhang, R. Wang, W. Li, F. Shen, B. Yang and Y. Ma, *Angew. Chem. Int. Ed*, 2014, **53**, 2119-2123.
51. W. Li, D. Liu, F. Shen, D. Ma, Z. Wang, T. Feng, Y. Xu, B. Yang and Y. Ma, *Adv. Funct. Mater*, 2012, **22**, 2797-2803.
52. Q. Qi, J. Qian, X. Tan, J. Zhang, L. Wang, B. Xu, B. Zou and W. Tian, *Adv. Funct. Mater*, 2015, **25**, 4171-4171.
53. Z. Ma, X. Meng, Y. Ji, A. Li, G. Qi, W. Xu, B. Zou, Y. Ma, G.-C. Kuang and X. Jia, *Dyes and Pigments*, 2019, **162**, 136-144.
54. X. Zhang, Z. Ma, Y. Yang, X. Zhang, X. Jia and Y. Wei, *J. Mater. Chem. C*, 2014, **2**, 8932-8938.
55. A. Li, N. Chu, J. Liu, H. Liu, J. Wang, S. Xu, H. Cui, H. Zhang, W. Xu and Z. Ma, *Materials Chemistry Frontiers*, 2019, **3**, 2768-2774.
56. X. Liu, A. Li, W. Xu, Z. Ma and X. Jia, *PCCP*, 2018, **20**, 13249-13254.
57. L. Huang, L. Liu, X. Li, H. Hu, M. Chen, Q. Yang, Z. Ma and X. Jia, *Angew. Chem. Int. Ed.*, 2019, **58**, 16445-16450.
58. J. Wu, J. Tang, H. Wang, Q. Qi, X. Fang, Y. Liu, S. Xu, S. X.-A. Zhang, H. Zhang and W. Xu, *J. Phys. Chem. A*, 2015, **119**, 9218-9224.
59. J. Wu, H. Wang, S. Xu and W. Xu, *J. Phys. Chem. A*, 2015, **119**, 1303-1308.

For Table of Contents use only:

View Article Online
DOI: 10.1039/D0CP02783A

Multicolored Fluorescence Variation of a New Carbazole-Based AIEE Molecule by External Stimuli

Yan Liu,[ae] Aisen Li,[be] Zhimin Ma,[c] Weiqing Xu,[b] Zhiyong Ma,*[a] and Xinru Jia[d]

In this article, we design and synthesize a new carbazle-based molecule Cz2CN with twisted D-A structure, using carbazole group as the donor and dicyanoethylene fragment as the acceptor. The twisted D-A structure endows Cz2CN with two characteristic emission bands, LE emission and ICT emission. Cz2CN is enabled with AIEE, solvatochromism, different response to anisotropic shearing force and isotropic hydrostatic pressure, due to the sensitivity of ICT emission to aggregation, solvent polarity and mechanical force. Aggregation benefits the ICT emission, leading to the AIEE of Cz2CN in THF/water system. Polar solvent can help stabilize the ICT excited states and enhance the ICT emission. The original crystalline powder is strongly fluorescent with high quantum yield of 40.4%. The single crystal of Cz2CN is obtained and dimers without π-π interactions among carbazole groups contribute to the strong emission. Anisotropic shearing alters the emission of Cz2CN powder from sky blue (474 nm) to green (520 nm). The single crystal of Cz2CN undergoes a distinct multicolored variation from sky-blue (476 nm) to green (510 nm) and further to orange (590 nm) by isotropic hydrostatic pressure. The emission of the original powder/crystal is dominant by LE emission in HLCT. Upon force/pressure, the ICT emission becomes dominated and red-shifts progressively. To the best of our knowledge, Cz2CN is a rare carbazole-based molecule that shows simultaneous AIEE, solvatochromism and force-induced multicolored variation.